Oil Shale, 2018, Vol. 35, No. 1, pp. 1–25
doi: https//doi.org/10.3176/oil.2018.1.01
ISSN 0208-189X

CHARACTERISTICS AND ACCUMULATION OF MIDDLE JURASSIC OIL SHALE IN THE YUQIA AREA, NORTHERN QAIDAM BASIN, NORTHWEST CHINA

QINGTAO MENG[(a,b)*], ZHAOJUN LIU[(a,b)*], PINGCHANG SUN[(a,b)], YINBO XU[(c)], FENG LI[(c)], YUEYUE BAI[(a,b)], WENQUAN XIE[(a,b)], SHUO DENG[(a,b)], SHUO SONG[(a,b)], KEBING WANG[(a,b)], CHUAN XU[(a,b)]

[(a)] College of Earth Sciences, Jilin University, Changchun 130061, China
[(b)] Key-Lab for Oil Shale and Paragenetic Minerals of Jilin Province, Changchun 130061, China
[(c)] Center of Oil and Gas Resources Survey, China Geological Survey, Beijing 100029, China

Abstract. *Two oil shale sequences in the Middle Jurassic Shimengou Formation in the Yuqia area, northern Qaidam Basin in Northwest China were evaluated based on geochemical and proximate analyses. The characteristics and accumulation conditions of oil shale in the Lower Coal-bearing Member (J_2sh^1) and Upper Shale Member (J_2sh^2) are different. The oil shale in J_2sh^1 with a high, terrigenous organic matter (OM)-derived total organic carbon (TOC) content is of medium-high oil yield, low ash and moisture contents, and low-medium calorific value and sulfur content. The oil shale in J_2sh^2 having a medium, alginite and bituminite-originated TOC content is characterized by a low-medium oil yield, high ash content, and low calorific value and moisture and sulfur contents. The oil shale in J_2sh^1 was deposited in a limnic environment under a varied climate from hot-humid to warm-humid, whereas that in J_2sh^2 was deposited in a semi-deep and deep lake environment under a stable warm-humid climate. Climatic conditions may have controlled the quality, distribution and thickness of oil shale by influencing the origin of organic matter and sedimentary environment. High paleoproductivity in J_2sh^2 (or high terrigenous detrital matter input in J_2sh^1) and strong water salinity stratification are responsible for the accumulation of high-quality oil shale.*

Keywords: *oil shale geochemical characteristics, industrial quality, accumulation conditions, Middle Jurassic, Qaidam Basin.*

[*] Corresponding authors: e-mail *mengqt@jlu.edu.cn*; *liuzj@jlu.edu.cn*

1. Introduction

Oil shale deposits in China range widely in age from the Late Paleozoic to the Cenozoic, while Mesozoic oil shale resources are most abundant, accounting for 84% of the country's total oil shale resources [1]. The Jurassic and Cretaceous were the most important periods of oil shale accumulation, while Middle Jurassic oil shale deposits are mostly distributed in western China and Cretaceous oil shale is distributed in eastern China. Previous exploration and studies mainly focused on Cretaceous oil shale in the Upper Cretaceous Songliao and Lower Cretaceous Luozigou and Laoheishan basins; the characteristics, depositional environment and metallogenic mechanism of oil shale in these basins have been thoroughly investigated by a number of scholars [2–7]. However, little research on the characteristics and accumulation of Middle Jurassic oil shale has been reported [8, 9].

The Qaidam Basin is the third largest inland basin of China, and covers approximately 250,000 km^2. It has attracted attention because of abundant salt, natural gas and coal resources [10, 11] and is the seventh largest oil shale-bearing basin in China with total Middle Jurassic oil shale resources of 16.8 billion tons [12]. The Yuqia oil shale-bearing area, which is situated in the central part of the northern Qaidam Basin, has abundant oil shale resources. However, little exploration has currently been undertaken for oil shale resources in this vast area, likely due to a poor understanding of the characteristics and accumulating mechanisms of oil shale therein.

The aim of the present research was to systematically study the geochemical and industrial characteristics of Middle Jurassic oil shale in the Yuqia area of the northern Qaidam Basin. Another goal was to investigate the climatic conditions and sedimentary environment of oil shale accumulation, and then further reveal the factors controlling the distribution and quality of oil shale. This study will improve the understanding of the accumulation mechanism of Middle Jurassic oil shale in the northern Qaidam Basin, and further promote oil shale exploration in the area.

2. Geological setting

The Qaidam Basin is located at the northeastern margin of the Tibetan Plateau in Northwest China (Fig. 1a). It is offset by the NEE-striking strike-slip Altyn Tagh Fault in the northwest, cut by the NW-striking strike-slip Elashan Fault in the east, and bounded by the Northern Kunlun Fault in the south (Fig. 1b). The Qaidam Basin is a Mesozoic and Cenozoic intracontinental basin that developed on the Precambrian crystalline basement [13]. The tectonic division of the northern Qaidam Basin is divided into the northern fault block belt (I) in the west and the Delingha Depression (II) in the east. The basin is also composed of multiple mosaic-distributed secondary structural belts, depressions and bulges (Fig. 1c) [14, 15].

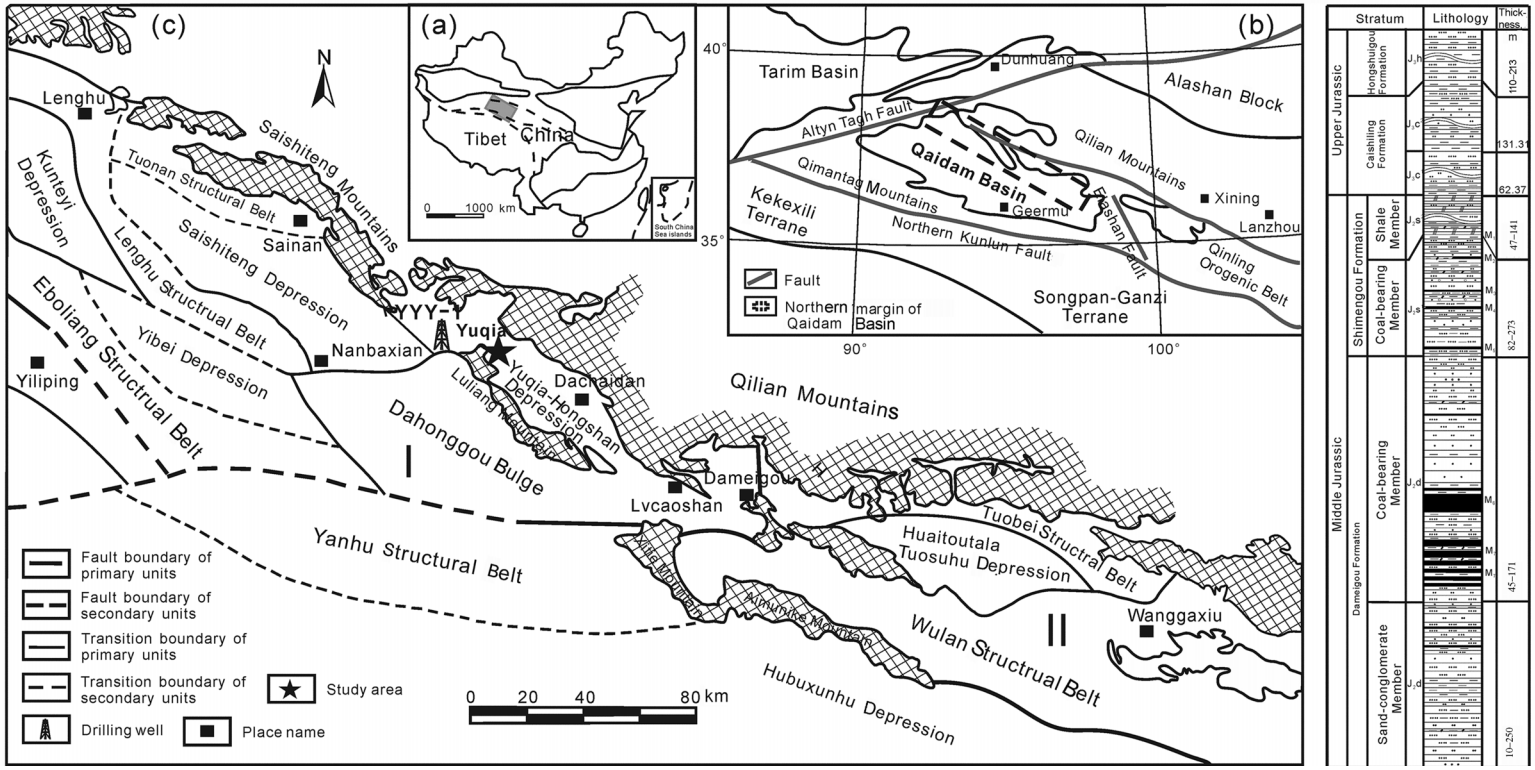

Fig. 1. (a) Location of the Qaidam-Qilian Mountains Basin system in China; (b) tectonic location of the Qaidam Basin (modified after [14, 15]); (c) tectonic division of the northern Qaidam Basin and the location of the study area and the sampling well (modified after [14, 15]); (d) stratigraphic characteristics of Middle Jurassic oil shale, northern Qaidam Basin.

The Yuqia oil shale-bearing area is situated in the Yuqia-Hongshan Depression in the central part of the northern fault block belt, between the Qilian and Luliang Mountains, and has an area of 500 km^2 (Fig. 1c). The Middle Jurassic (coal and oil shale-bearing) stratum is up to 1 km thick, comprising Dameigou and Shimengou Formations, of which, the latter is the main oil shale-bearing layer. This formation is divided into the Lower Coal-bearing Member and the Upper Shale Member. The Coal-bearing Member is dominated by gray-gray black siltstone, silty mudstone and carbonaceous shale and is intercalated with coal seams (M1–M5), while coal seam M5 is recoverable throughout the area. The overlying Shale Member is composed of brown, dark gray shale and oil shale in the lower part and grayish-green mudstone and siltstone in the upper part (Fig. 1d).

3. Materials and methods

The fully cored borehole YYY-1 was drilled in 2015 in the western part of the Yuqia oil shale-bearing area. Bulk organic geochemical, Fischer assay (FA) and proximate analyses were performed in the depth intervals of 330–390 m and 470–562 m, using a composite samples representative for a 1-m-thick interval. In addition, 53 point samples were chosen for inorganic geochemical analysis and 16 point samples were collected for polished section preparation. The samples were mostly oil shale, coal, mudstone, silty mudstone and siltstone.

Fischer assay oil yield (wt%), Rock-Eval parameters, total organic carbon (TOC, wt%) and sulfur content were determined and proximate analysis was performed at the Key-Lab for Oil Shale and Paragenetic Minerals of Jilin Province, Changchun, China. Oil yield gained from low-temperature carbonization at approximately 520 ^oC was measured using a Chinese Fushun retort, by FA. The mixture of oil and water was extracted from oil shale by heating, and the content of oil was obtained by weighting the water distilled from the mixture. Afterwards, the oil yield was calculated from the total weight. TOC was measured using a Leco CS-230 elemental analyzer on samples pre-treated with concentrated HCI. Rock-Eval pyrolysis was carried out employing a Rock-Eval 6 instrument. With this method, the quantity of pyrolyzate (mg HC/g rock) generated from kerogen during gradual heating in a helium stream is normalized to TOC to give the hydrogen index (HI, mg HC/g TOC). The temperature of maximum product generation (T_{max}) serves as a maturation indicator. Ash yield, moisture and volatile contents as well as gross calorific value were determined following Chinese standard methods GB/T 212-2008 [16] and GB/T 213-2008 [17]. A polished section was used for microscopic investigations. Maceral analysis was performed employing a single-scan method [18], with a Leica MPV microscope using reflected white and fluorescent light.

Major element oxide and trace element contents were determined using a Philips PW2404 X-ray fluorescence (XRF) spectrometer and a Thermo Scientific X-Series high resolution inductively coupled plasma mass spectrometer (HR-ICP-MS) at the Beijing Research Institute of Uranium Geology, China, following the criteria of Chinese national standards GB/T 14506.28-93 [19] and DZ/T 0223-2001 [20], respectively.

4. Characteristics of oil shale

4.1. Lithological characteristics

The oil shale of the Shimengou Formation in the Yuqia area is a mudstone-type oil shale. It is mainly gray-brown, gray-black or black in colour, and has developed flat and massive beddings. This high-quality oil shale can be ignited directly. Shell and fish fossils can be observed in it.

Two types of rock associations between oil shale-bearing layers can be identified. One is revealed by that gray black-black oil shale, which is distributed in the Lower Coal-bearing Member of the Shimengou Formation (J_2sh^1) (Fig. 2), mostly occurs with black coal and gray-black carbonaceous shale. The other consists in that gray-brown oil shale, which is distributed in the Upper Shale Member of the Shimengou Formation (J_2sh^2) (Fig. 3), occurs together with dark gray mudstone, silty mudstone and siltstone.

4.2. Organic geochemical characteristics

4.2.1. Bulk geochemical parameters

Bulk geochemical data about the studied oil shale samples are given in Table 1.

4.2.1.1. Coal-bearing Member (J_2sh^1)

High TOC values were measured in the oil shale sample from J_2sh^1, ranging from 13.8 to 48.8 wt% (average 25.6 wt%) (Table 1, Fig. 2a). The hydrogen index (HI) values varied between 267 and 385 mg HC/g TOC (Fig. 2b). Plots of HI vs T_{max}, HI vs oxygen index (OI), and S_2 vs TOC show that the oil shale comprises Type II_2 kerogen (Fig. 4), having a certain contribution of terrestrial organic matter (OM). T_{max} values varied between 424 and 429 °C, reflecting that the rock is immature.

4.2.1.2. Shale Member (J_2sh^2)

The TOC content of the oil shale sample from J_2sh^2 was significantly lower than that of the sample from J_2sh^1, varying from 1.76 to 13.7 wt% (average 8.0 wt%) (Table 1, Fig. 3a). At the same time, HI was typically between 511 and 982 mg HC/g TOC (Table 1, Fig. 3b), being higher than that of the sample from J_2sh^1. Most samples plot in the fields that are characteristic for

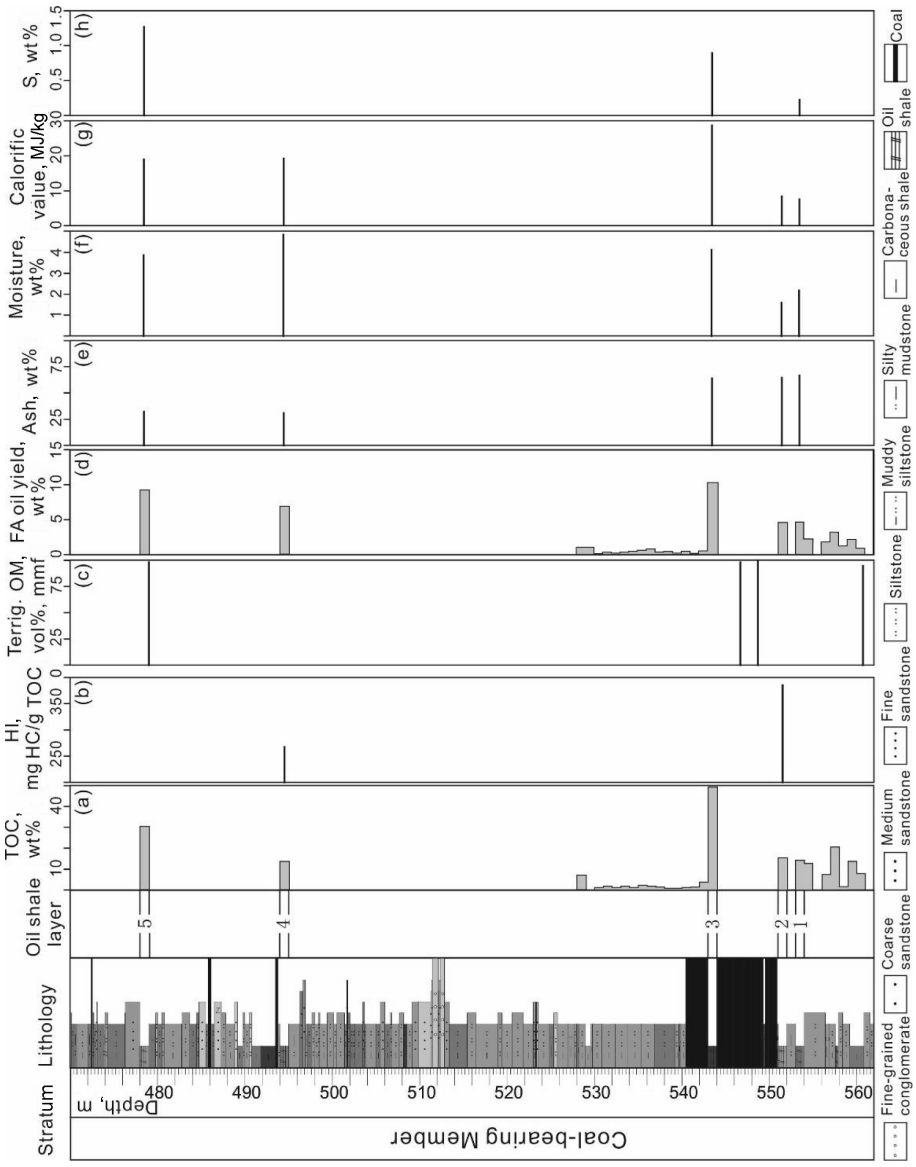

Fig. 2. Depth profiles of bulk geochemical proxies, organic macerals and industrial parameters of oil shale in the Coal-bearing Member, Shimengou Formation, Qaidam Basin. Oil shale layers are numbered from bottom to top. (Abbreviations: TOC – total organic carbon; HI – hydrogen index; S – sulfur; Terrig. OM – terrigenous organic matter; mmf – magneto-motive force.)

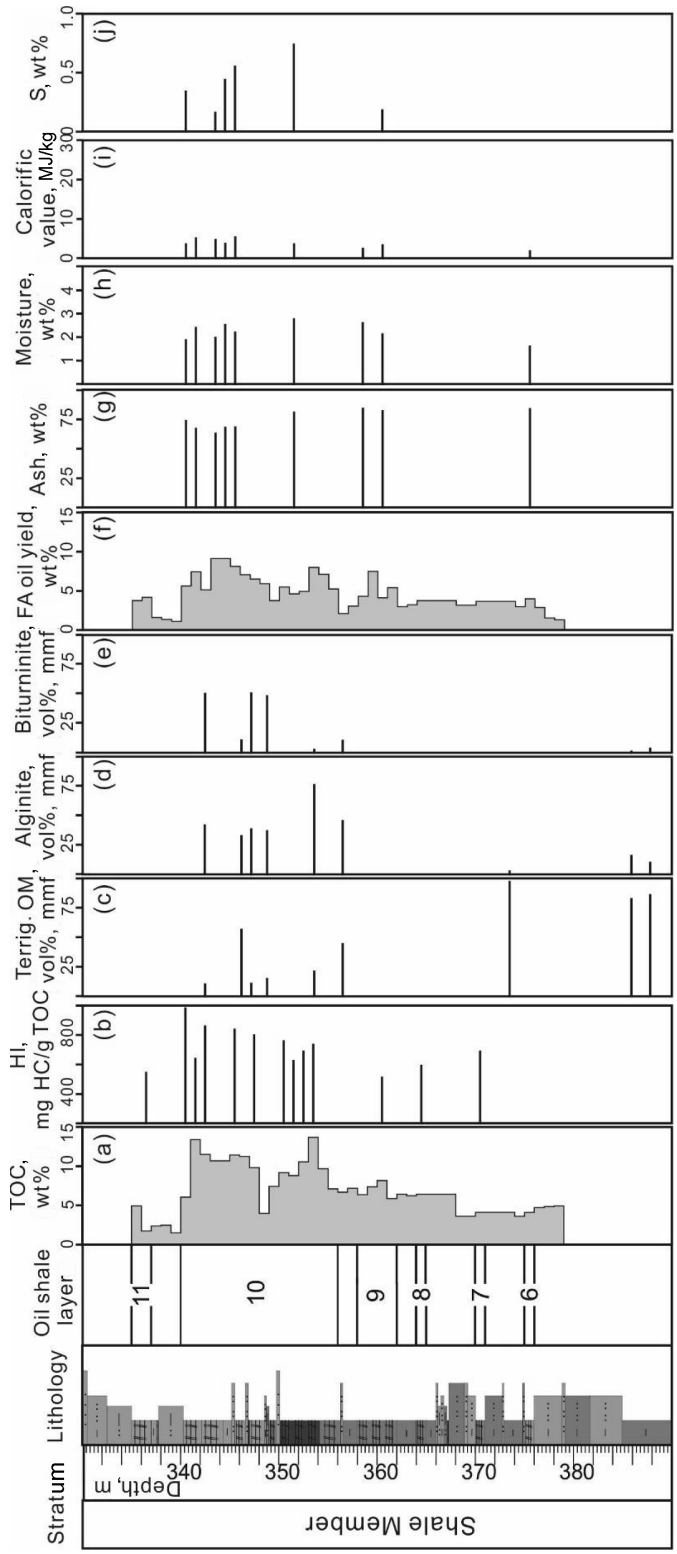

Fig. 3. Depth profiles of bulk geochemical proxies, organic macerals and industrial paramters of oil shale in the Shale Member, Shimengou Formation, Qaidam Basin. Oil shale layers are numbered from bottom to top. (Abbreviations: TOC – total organic carbon; HI – hydrogen index; S – sulfur; Terrig. OM – terrigenous organic matter; mmf – magnetomotive force.)

Table 1. Organic geochemical and industrial characteristics of oil shale in the northern Qaidam Basin

Formation		Oil shale layer	Depth, m	Thickness, m	TOC, wt%		HI, mg HC/g TOC	T_{max}, °C	Oil yield (FA), wt%		Gas and loss, wt%	Ash, wt%	Water, wt%	Volatile, wt%	Fixed carbon, wt%	Calorific value, MJ/kg	Sulfur, wt%	Density, g/cm^3
					Min.–max.	Average	Min.–max.	Min.–max.	Min.–max.	Average	Min.–max.	Min.–max.	Min.–max.	Min.–max.	Min.–max.	Min.–max.	Min.–max.	
Shimengou Formation	Shale Member	11	335–337	2	1.76–4.97	3.36	544	429	3.79–4.24	4.02	0.99–2.33	75.74	1.38	23.00	0.04	2.92	—	—
		10	340–356	16	4.01–13.7	9.46	626–982	430–441	3.80–9.17	6.18	1.38–4.49	62.9–81.0	1.86–2.76	15.62–35.18	0.01–0.62	3.54–5.36	0.16–0.74	1.81–2.13
		9	358–362	4	5.92–8.22	6.99	511	435	4.35–7.5	5.37	1.05–3.08	82.02–84.14	2.12–2.59	13.26–14.53	0.01-1.33	2.39–3.33	0.18	1.99
		8	364–365	1	–	6.44	593	437	–	3.75	1.58	–	–	–	–	–	–	–
		7	370–371	1	–	4.14	688	435	–	3.71	1.28	–	–	–	–	–	–	–
		6	375-376	1	–	4.15	–	–	–	4.02	4.35	83.54	1.59	14.77	0.11	1.87	–	–
	Coal-bearing Member	5	478–479	1	–	33.5	–	–	–	9.3	4.69	33.17	3.86	59.32	3.64	18.80	1.27	2.17
		4	494–495	1	–	16.8	267	424	–	6.99	5.37	31.66	4.85	34.86	28.62	19.02	–	–
		3	543–544	1	–	48.8	–	–	–	10.35	8.19	64.16	2.12	28.23	5.49	28.50	0.90	1.11
		2	551–552	1	–	15.15	385	429	–	4.63	13.76	65.07	1.59	21.17	12.17	8.36	–	–
		1	553–554	1	–	13.8	–	–	–	4.71	4.12	67.17	2.17	18.77	11.88	7.43	0.23	2.22

Note: "—" represents no data.

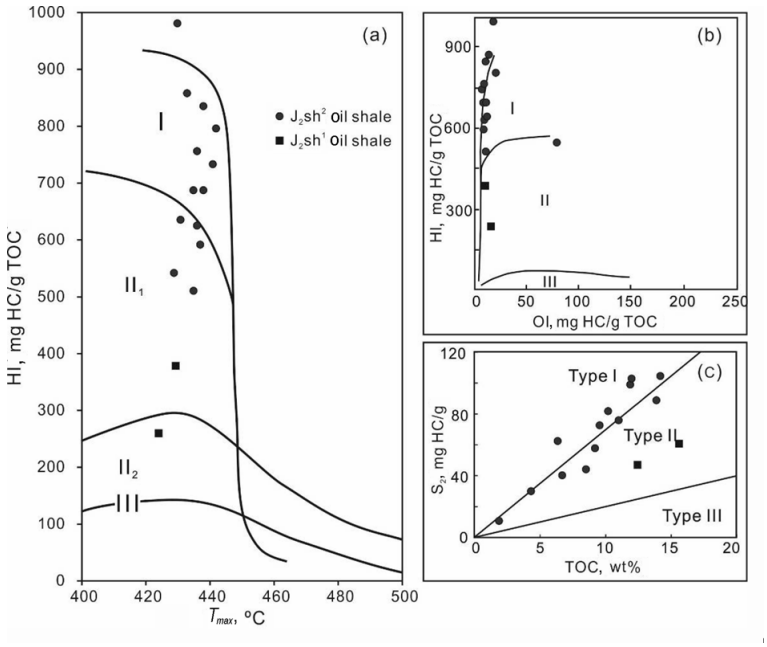

Fig. 4. Plot of HI vs T_{max}, HI vs OI (according to [17]) and S_2 vs TOC (according to [18]) outlining kerogen types of oil shales from the Shimengou Formation, Qaidam Basin. (Abbreviations: HI – hydrogen index; OI – oxygen Index.)

Type I and II_1 kerogens (Fig. 4), indicating the predominance of lacustrine OM. T_{max} values varied between 429 and 442 °C, suggesting that the oil shale is immature or at the low-maturity stage of thermal evolution.

4.2.2. Organic petrography

The component variation of terrigenous organic matter and the sum of vitrinite, inertinite, sporinite, resinite, cutinite, fluorinite, and alginite (the sum of lamalginite and telalginite, Table 2) are plotted respectively in Figure 2c and Figure 3c–d.

Oil shale, dark mudstone and coal samples were selected for organic maceral analysis in this study. The rocks were shown to differ in OM type. The oil shale samples from J_2sh^2 were characterized by the relatively high contents of alginite (average 46 vol%) and biturninite (average 25 vol%) (Fig. 3d–e). Lamalginite predominates over telalginite in the majority of oil shale samples. Lamalginite may originate from assemblages of algae and bacteria. Telalginite includes solitary and colonial algae [21]. Biturninite may be decomposed from algae, plankton and bacterial lipids. Black mudstone samples were mostly composed of terrigenous OM (83–97 vol%) (Fig. 3c). Sporinite (average 50 vol%) and vitrinite (average 23 vol%) are dominating (Table 2). This indicates that aquatic organisms were the primary

Table 2. Organic petrology and vitrinite reflectance data about samples from the Shimengou Formation, Yuqia area, northern Qaidam Basin

Stratum	Sample	Lithology	Depth, m	Alginite, vol%, mmf		Terrigenous organic matter, vol%, mmf					Bituminite, vol%, mmf	Vitr. refl., %Rr
				telalginite	lamalginite	sporinite	cutinite	fluorophor	vitrinite	inertinite		
Shale Member	OP-1	Black oil shale	336.5	33.74	9.20	49.08	3.07	1.23	0.61	0.00	3.07	0.61
	OP-2	Black oil shale	342.5	0.00	39.92	1.38	0.00	0.20	6.92	1.58	50.00	–
	OP-3	Black oil shale	346.2	2.04	30.55	36.66	4.89	4.07	8.76	2.24	10.79	–
	OP-4	Black oil shale	347.2	9.59	28.98	8.28	0.44	0.87	0.00	1.09	50.76	0.61
	OP-5	Black oil shale	348.8	4.57	32.18	2.19	0.55	0.18	10.79	1.28	48.26	–
	OP-6	Black oil shale	353.6	6.87	69.31	4.08	0.43	0.21	13.73	2.58	2.79	–
	OP-7	Black oil shale	356.5	1.57	44.03	22.33	8.81	3.46	7.86	1.89	10.06	0.55
	OP-8	Black mudstone	373.5	1.27	1.27	75.95	1.27	3.80	15.19	1.27	0.00	–
	OP-9	Black mudstone	385.9	12.82	3.42	58.12	17.09	1.71	4.27	1.71	0.85	–
	OP-10	Black mudstone	387.8	10.17	0.00	18.40	15.98	6.05	39.23	6.54	3.63	–
	OP-11	Gray mudstone	405.4	12.64	0.00	31.77	4.38	0.00	40.52	10.05	0.65	–
	OP-12	Gray mudstone	410.7	3.31	0.00	66.23	6.62	5.96	13.91	3.31	0.66	–
Coal-bearing Member	OP-13	Black oil shale	479.0	1.85	0.00	9.76	13.46	2.11	70.45	2.37	0.00	–
	OP-14	Black coal	546.7	1.78	0.00	1.39	0.00	0.00	94.65	2.18	0.00	–
	OP-15	Black coal	548.7	0.43	0.00	0.22	0.00	0.00	96.97	2.38	0.00	–
	OP-16	Black mudstone	560.8	2.20	0.00	11.58	2.99	1.00	73.15	6.09	2.99	0.55

Note: "—" represents no data; mmf – momentomagnetic force; Vitr. refl. – vitrinite reflectance.

producers of OM during the deposition of oil shale in J_2sh^2, whereas the mixture of aquatic and terrigenous OM was the dominant primary producer of black mudstone.

Almost all samples of oil shale, coal and mudstone from J_2sh^1 were predominated by terrigenous OM (> 95 vol%) (Fig. 2c). The most abundant OM component was vitrinite (average 84 vol%), while coal samples stood out with its highest percentage, 97 vol% (Table 2).

4.3. Industrial quality characteristics

Oil yield, and ash, moisture and sulfur contents, as well as calorific value and density are key parameters for oil shale resource evaluation and utilization [12].

4.3.1. Oil yield

FA oil yields of the two oil shales were different. The oil yield of oil shale of J_2sh^1 varied from 4.7 to 10.4 wt%, the highest yield (10.4 wt%) was obtained from the sample from the 1-m thick layer 3 (Fig. 2d). The oil yield of oil shale of J_2sh^2 was slightly lower, ranging from 3.79 to 9.17 wt%. The highest oil yield (9.17 wt%) was obtained from the sample from the 1-m thick oil shale layer 10, with a total thickness of 16 m (Table 1, Fig. 3f).

Plots of oil yield vs TOC of all samples of oil shale, mudstone, coal and carbonaceous shale showed a strong positive correlation with R^2 of 0.89 in J_2sh^1, and a moderate positive correlation with R^2 of 0.62 in J_2sh^2. These results indicate that the samples from J_2sh^1 with TOC > 14.1 wt% can be considered oil shale (FA > 3.5wt%), and the samples from J_2sh^2 with TOC > 4.8 wt% can also be considered oil shale (FA > 3.5wt%). Therefore, TOC can serve as a valuable alternative indicator of the oil yield of oil shale from the Yuqia area.

4.3.2. Ash content

Oil shale ash is the residue deriving from the rock inorganic and organic matter during combustion. Ash content is an important indicator to distinguish between oil shale and coal. The ash content of Chinese oil shale is generally less than 40 wt% [12]. The oil shale sample from J_2sh^1 had an ash yield from 31.7 to 67.2 wt% (average 52.3 wt%) (Table 1, Fig. 2e), therefore it can be considered low-ash oil shale. Conversely, the ash yield of the oil shale sample from J_2sh^2 was between 62.9 and 84.1 wt% (average 74.7 wt.%) (Table 1, Fig. 3g), and thus this rock can be regarded as high-ash oil shale.

4.3.3. Moisture content

Moisture content is a basic parameter to assess the feasibility of oil shale mining, processing and combustion. When its moisture content is higher

than 25 wt%, oil shale should be dried in advance, which will increase production costs. According to moisture content, oil shales can be divided into high- (> 20–30 wt%), medium- (10–20 wt%) and low-moisture (< 10 wt%) oil shales [22]. The moisture content in the oil shale samples from J_2sh^1 ranged from 1.59 to 4.85 wt% (Table 1, Fig. 2f), which is slightly higher than the 1.38–2.76 wt% range in those from J_2sh^2 (Table 1, Fig. 3h), however, both can be considered low-moisture oil shales.

4.3.4. Calorific value

Calorific value is an important parameter to evaluate the combustion value of oil shale [12]. As seen from Table 1, the calorific values of oil shale samples from J_2sh^1 and J_2sh^2 varied from 7.43 to 28.5 MJ/kg and from 1.87 to 5.36 MJ/kg, respectively (Fig. 2g, Fig. 3i).

4.3.5. Sulfur content

Sulfur content refers to the sum total of the contents of all types of sulfur in oil shale, including organic and inorganic sulfur. During combustion, organic sulfur is nearly entirely emitted into the atmosphere as aerosols and gaseous products of flue gas emissions. SOx emissions may have a noxious effect on air, water and living organisms, including humans [23]. Thus, sulfur content is an important indicator for evaluating the potential environment pollution during the utilization of oil shale [12]. The sulfur content of the oil shale sample from J_2sh^1 varied between 0.23 and 1.27 wt%, indicating the rock to be a low-medium sulfur oil shale, while the sulfur content of the sample from J_2sh^2 was very low, ranging from 0.16 to 0.74 wt%, indicating it to be a low-sulfur oil shale (Table 1, Fig. 2h, Fig. 3j).

4.3.6. Density

Density is a key parameter to calculate oil shale resources. As seen from Table 1, the densities of oil shale samples from J_2sh^1 and J_2sh^2 slightly differ, being from 1.11 to 2.22 g/cm^3 and from 1.81 to 2.13 g/cm^3, respectively.

In summary, the industrial-quality oil shale sample from J_2sh^1 has a medium-high oil yield, low ash and moisture contents, and low-medium calorific value and sulfur content, whereas that from J_2sh^2 is characterized by a low-medium oil yield, high ash content, and low moisture and sulfur contents and calorific value.

5. Depositional environment and its control over oil shale accumulation

5.1. Paleoclimatic conditions

Paleomagnetic data show that the Qaidam Basin was located in the north latitude 8.8° during the Early Middle Jurassic [24]. The pollen assemblage

was dominated by *Inaperturopollenites*, *Psophosphaera* and *Cyathidites*, and the *Classopollis* content was decreased, indicating that the vegetation was subtropical mixed forest [25].

The chemical index of alteration (CIA = $[Al_2O_3/(Al_2O_3 + CaO^* + Na_2O + K_2O)] \times 100$) and a similar index ($CIA_{(molar)} = Al_2O_{3(molar)}/(CaO^*_{(molar)} + Na_2O_{(molar)} + K_2O_{(molar)})$) can be used to reflect paleoclimatic conditions [26, 27]. In these equations all values are in molar proportions. CaO* represents the amount of CaO incorporated into the silicate fraction of the rock. It is calculated using the equation $CaO^* = CaO - (10/3 \times P_2O_5)$ to correct CIA for P_2O_5 (apatite). If the result of the mole fraction of CaO is greater than that of Na_2O, then CaO* is equal to Na_2O. Otherwise, CaO* is equal to CaO [26]. Generally, CIA values between 65 and 85 correspond to a warm and humid climate, whereas values between 85 and 100 correspond to a hot and humid tropical and sub-tropical climate [24].

Plots of $CIA_{(molar)}$ and Al_2O_3 and K_2O/Na_2O of samples indicate that the oil shale of the Shimengou Formation was deposited in a subtropical climate (Fig. 5). The CIA values of samples from J_2sh^1 were between 75 and 94 (average 84) (Table 3), and the vertical curve reflects two climatic cycles from a hot-humid to warm-humid climate (Fig. 6b). Coal and high-quality oil shale in layer 3 (oil yield 10.35 wt%), layer 4 (oil yield 6.99 wt%) and layer 5 (oil yield 9.3 wt%) (CIA 75–82) were deposited in a warm and humid climate, whereas poor-quality oil shale in layer 1 (oil yield 4.71 wt%)

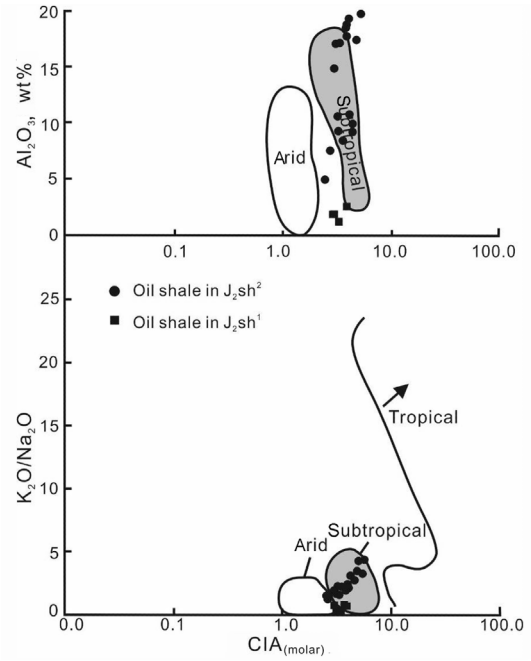

Fig. 5. Plots of CIA_{molar}, K_2O/Na_2O and Al_2O_3 (after [25]), illustrating deposition of oil shale in a subtropical climate.

Table 3. Typical major elements and respective ratios of samples from the Shimengou Formation, Yuqia area, northern Qaidam Basin

Sample	Depth, m	SiO_2, %	Al_2O_3, %	CaO, %	Na_2O, %	K_2O, %	Ca/Fe+Ca	Ba/Al	CIA	$CIA_{(molar)}$
Shale Member										
Y1	335.7	22.82	9.27	19.94	0.25	1.10	0.75	190.7	82	4.58
Y2	336.5	24.7	9.96	16.08	0.26	1.21	0.71	187.8	82	4.59
Y3	337.6	45.66	17.48	7.61	0.35	2.20	0.55	107.4	83	4.96
Y4	338.6	45.55	17.37	9.08	0.37	2.16	0.61	108.1	83	4.89
Y5	340.7	29.25	10.81	18.23	0.32	1.35	0.72	117.1	81	4.29
Y9	343	26.62	7.58	19.47	0.44	1.12	0.85	290.6	74	2.86
Y10	344	29.18	9.30	19.57	0.44	1.22	0.82	322.1	77	3.37
Y11	345.9	25.13	8.48	23.74	0.35	1.07	0.87	192.5	79	3.69
Y12	347.2	21.1	4.99	31.73	0.36	0.73	0.87	337.7	72	2.55
Y13	348.8	54.14	17.14	0.80	0.80	2.52	0.16	137.3	76	3.20
Y14	350.23	41.44	10.65	11.70	0.53	1.36	0.73	205.0	77	3.32
Y16	352.5	51.52	17.18	0.67	0.74	2.35	0.10	160.5	78	3.45
Y17	353.6	49.64	14.92	0.79	0.80	2.04	0.15	126.3	75	3.07
Y18	355.2	51.78	17.82	0.49	0.68	2.24	0.10	100.5	80	4.02
Y20	358.3	54.95	18.89	0.54	0.63	2.39	0.11	121.2	80	4.11
Y21	360.3	53.39	18.53	0.48	0.67	2.47	0.06	122.5	80	3.98
Y23	364.7	53.89	19.33	0.39	0.58	2.69	0.06	110.8	81	4.22
Y24	368.3	54.07	21.27	0.51	0.51	2.54	0.11	104.8	83	4.80
Y25	370.1	53.77	20.88	0.35	0.50	2.62	0.07	105.1	83	4.84
Y28	374.23	47.19	19.77	0.62	0.43	2.08	0.05	103.4	84	5.39
Y30	377.7	45.86	20.38	0.61	0.35	2.27	0.05	96.6	85	5.65
Coal-bearing Member										
Y-32	469.2	8.9	3.94	0.34	0.18	0.28	0.50	–	82	4.49
Y34	479	3.72	1.79	3.22	0.14	0.13	0.47	–	75	2.95
Y37	494.7	3.12	1.87	0.19	0.15	0.14	0.08	–	75	2.98
Y40	503.2	59.5	23.76	0.20	0.23	2.92	0.08	–	86	6.06
Y43	516.8	58.28	22.78	0.21	0.22	2.64	0.05	–	86	6.36
Y44	524.3	53.87	22.31	0.30	0.26	2.39	0.10	–	87	6.46
Y46	534.3	48.43	21.17	0.61	0.18	2.25	0.04	–	87	6.97
Y49	547.7	1.44	1.19	0.30	0.10	0.04	0.42	–	77	3.33
Y51	552.7	47.11	28.42	0.16	0.15	1.16	0.14	–	94	16.16
Y52	556.7	28.42	15.00	0.39	0.23	1.04	0.27	–	89	7.93

Note: "—" represents no data.

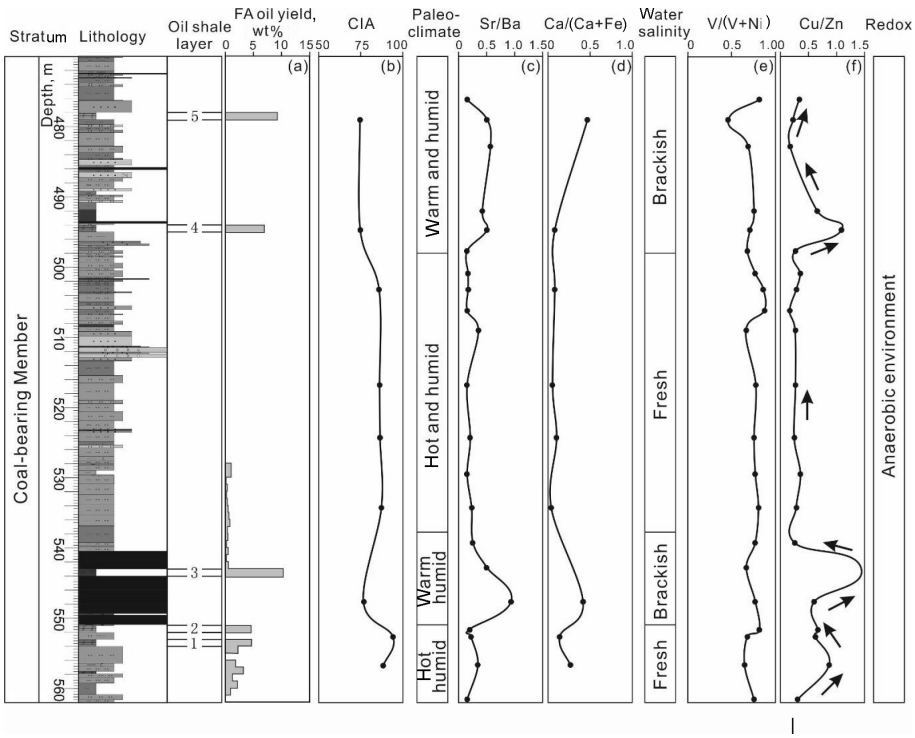

Fig. 6. The vertical variation of CIA and some element ratios in J_2sh^1, showing the change of paleoclimate, water salinity and redox conditions (the legend as in Fig. 3).

and layer 2 (oil yield 4.63 wt%) was accumulated in a relatively hot and humid climate (Fig. 6a–b). The CIA values of samples from J_2sh^2 varied from 74 to 85 (average 80) (Table 3), also implying a stable warm and humid paleoclimate. The values gradually decreased with an increase in oil yield from bottom to top (Fig.7a–b), indicating that the climate during the deposition of high-quality oil shale (layer 10) was warmer and more humid than during the accumulation of poor-quality oil shale.

These results suggest that climatic conditions controlled oil shale accumulation. In a warm and humid climate, significant runoff deposited sufficient nutrients into a lake, which was of benefit to the growth and reproduction of a variety of biological organisms. The lake's primary productivity was greatly increased, providing plenty of organic matter for oil shale formation. In addition, climate could also control lake level changes by influencing the balance between evaporation and recharge of lake water, to regulate the distribution and thickness of oil shale. The varying climate during the deposition of J_2sh^1 caused lake level fluctuations, resulting in the deposition of thin layers of oil shale and coal. In contrast, the stable warm and humid climate during the accumulation of J_2sh^2 formed thick layers of oil shale.

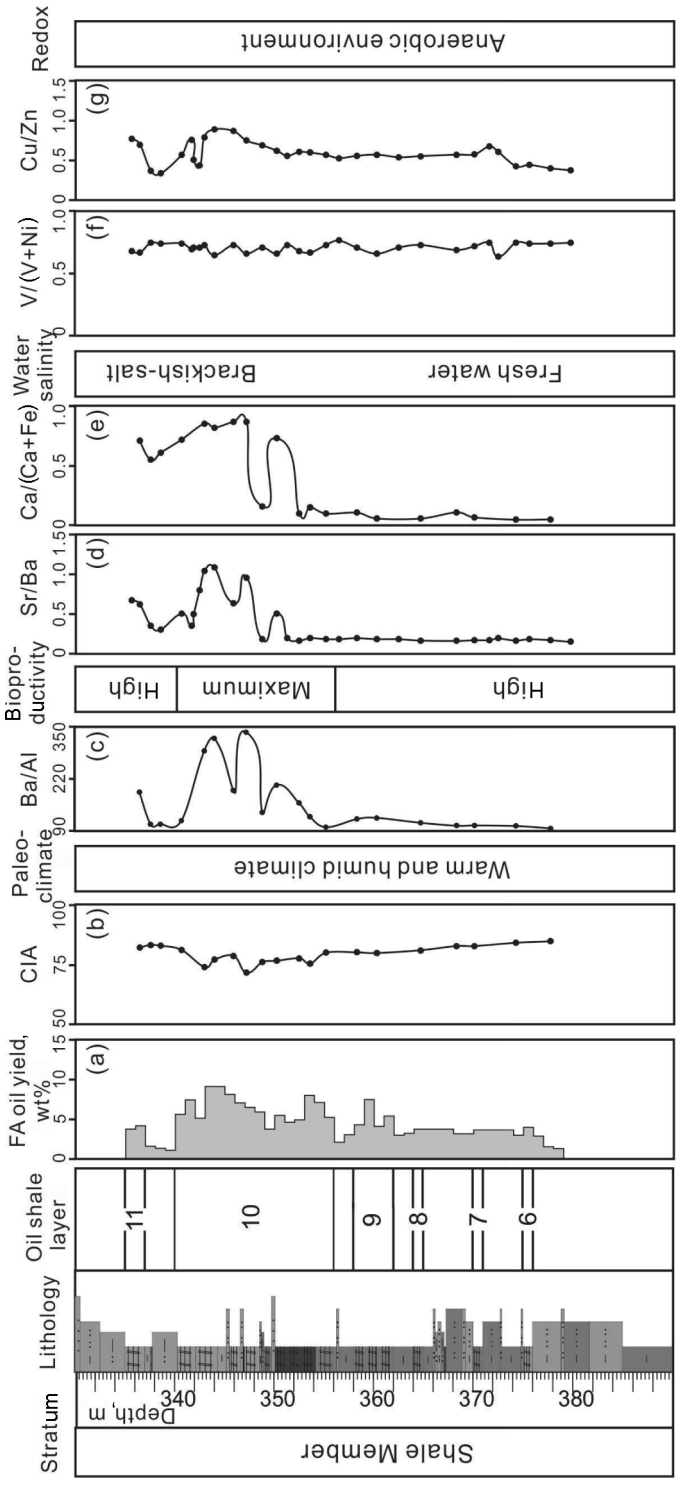

Fig. 7. The vertical variation of CIA and some element ratios in J_2sh^2, showing the change of paleoclimate, water salinity and redox conditions (the legend as in Fig. 3).

5.2. Sedimentary environment

Based on core observations and sedimentary facies analysis, the sedimentary evolution of the Shimengou Formation in the Yuqia area was revealed. During the depositional period of J_2sh^1, the Yuqia area was dominated by fan delta and lacustrine sediments. The deposits in the area adjacent to the basin center are fan delta plain, fan delta front and shallow lake, respectively (Fig. 8). The oil shale generally contacts coal at the top and base, mainly deposited in a limnic environment (Fig. 2). J_2sh^2 consists of sediments deposited in a lacustrine depositional system (Fig. 8), and is characterized by thick oil shale and dark mudstone with flat bedding (Fig. 3). Oil shale mainly developed in a semi-deep lake environment.

The sedimentary environment also controlled the distribution and thickness of oil shale. The varying sedimentary environment and limited limnic area of J_2sh^1 led to the uneven distribution of oil shale occupying small separate areas and being of small thickness. In contrast, the stable semi-deep lake environment of J_2sh^2 produced oil shale layers which are widely distributed across the region and are of greater thickness.

5.3. Origin of organic matter and paleoproductivity

Organic macerals and Rock-Eval data show the organic matter of J_2sh^1 oil shale to be Type II_2 kerogen (Fig. 4) of predominantly terrigenous origin (Fig. 2c), indicating that terrigenous detrital matter was the primary producer of OM of this oil shale. In contrast, the organic matter of J_2sh^2 oil shale is mainly Type I and II_1 kerogens (Fig. 4) and derived from aquatic organisms, including alginite and biturninite (Fig. 3d–e), which suggests that its formation was mostly influenced by lake paleoproductivity.

The trace element Ba generally has a positive correlation with the accumulation rate of organic carbon and paleoproductivity [28]. The Ba/Al ratio can, to a certain extent, mirror the amount of plankton of a geological period, indirectly reflecting lake paleoproductivity. Usually, a Ba/Al ratio between 100 and 120 suggests high paleoproductivity [29]. The Ba/Al ratio of J_2sh^2 oil shale varied from 96.6 to 337.7 (Table 3), reflecting a high paleoproductivity during deposition, while the paleoproductivity reached maximum during deposition of high-quality oil shale (layer 10) (Fig. 7c). These data give evidence of a close relationship between oil shale OM abundance and lake paleoproductivity. A higher productivity can result in the eutrophication of lake water, which is advantageous to the rapid spread of algae and other aquatic organisms, providing a good material basis for oil shale formation.

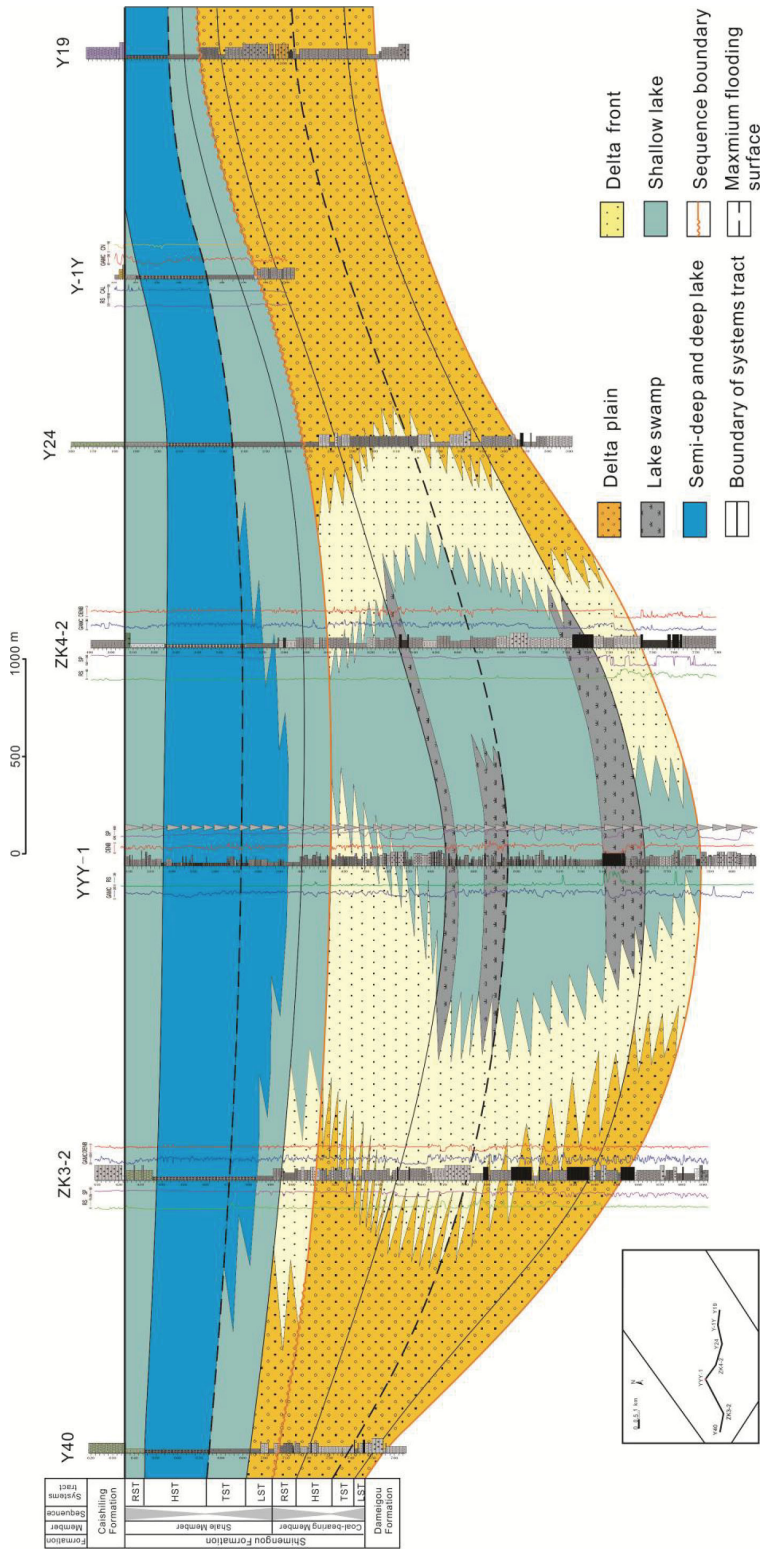

Fig. 8. Sequence-sedimentary connected well section from well Y40 to well Y19 of the Shimengou Formation in the Yuqia area, northern Qaidam Basin (Abbreviations: RST – regressive systems tract, HST – highstand systems tract, TST – transgressive systems tract, LST – lowstand systems tract.)

5.4. Lake water environment

5.4.1. Water salinity

Trace elements Sr and Ba and their ratio have proved to be good indicators of lake water salinity [30]. Generally, the Sr/Ba ratio in fresh water sediments is lower than 1, and in marine sediments, higher than 1. At the same time, in lacustrine environments without seawater intrusion, a Sr/Ba ratio between 0.5 and 1 refers to brackish water, while a value exceeding 1.0 is indicative of salty lake water in an arid climate [31, 32]. In J_2sh^1, the Sr/Ba ratio varied from 0.15 to 1.09, and a vertical curve is shown as two cycles changing from fresh to brackish water (Fig. 6c). High-quality oil shale and coal (Sr/Ba 0.5–0.94) were deposited in brackish water, whereas poor-quality oil shale (Sr/Ba 0.16–0.35) was deposited in fresh water (Fig. 6a and 6c). In the lower part of J_2sh^2, at a depth of 380 to 350.23 m, the Sr/Ba ratio is very low, between 0.16 and 0.20 (Table 4, Fig. 7d), and implies a fresh water environment. The ratio starts to increase toward the top of oil shale layer 11 (from 350 to 330 m), being for the majority of samples higher than 0.5, which signifies a brackish to salt water environment (Table 3, Fig. 7d).

Table 4. Typical trace elements and respective ratios of samples from the Shimengou Formation, Yuqia area, northern Qaidam Basin

Sample	Depth, m	Lithology	V, μg/g	Ni, μg/g	Cu, μg/g	Zn, μg/g	Sr, μg/g	Ba, μg/g	Sr/Ba	V/V+Ni	Cu/Zn
Shale Member											
Y1	335.7	Oil shale	87.6	40.9	44.6	58.2	320	468	0.68	0.68	0.77
Y2	336.5	Oil shale	97.4	46.9	52.6	75.6	310	495	0.63	0.67	0.70
Y3	337.6	Mudstone	89.5	29.4	31.1	84.4	178	497	0.36	0.75	0.37
Y4	338.6	Silty mudstone	88.1	31.7	31.1	92.2	152	497	0.31	0.74	0.34
Y5	340.7	Oil shale	90.1	31.1	33.5	58.5	170	335	0.51	0.74	0.57
Y6	341.7	Oil shale	125	52.8	61.3	80.8	181	500	0.36	0.70	0.76
Y7	341.9	Oil shale	85.2	34	34.6	68.4	183	369	0.50	0.71	0.51
Y8	342.48	Oil shale	42.8	17.9	16.6	38.1	243	303	0.80	0.71	0.44
Y9	343	Oil shale	71.7	26.9	37.9	47.7	610	583	1.05	0.73	0.79
Y10	344	Oil shale	104	55.3	51.6	58.2	864	793	1.09	0.65	0.89
Y11	345.9	Oil shale	104	38.8	45.2	52.2	276	432	0.64	0.73	0.87
Y12	347.2	Oil shale	62.7	31.7	23.3	31	426	446	0.96	0.66	0.75
Y13	348.8	Oil shale	134	53.5	75.6	110	119	623	0.19	0.71	0.69
Y14	350.23	Oil shale	96.4	49.7	49.7	80	292	578	0.51	0.66	0.62
Y15	351.3	Oil shale	112	41.2	52.4	92.8	106	518	0.20	0.73	0.56
Y16	352.5	Oil shale	137	63.2	69.9	115	125	730	0.17	0.68	0.61
Y17	353.6	Oil shale	84.4	40.8	42	69.5	98.5	499	0.20	0.67	0.60
Y18	355.2	Oil shale	121	45.6	53.2	92.6	89.4	474	0.19	0.73	0.57
Y19	356.5	Siltstone	129	38.7	55.6	104	101	531	0.19	0.77	0.53
Y20	358.3	Oil shale	141	57.7	69.4	125	120	606	0.20	0.71	0.56
Y21	360.3	Oil shale	139	72.8	62.8	111	115	601	0.19	0.66	0.57
Y22	362.5	Mudstone	138	56.3	61.2	114	106	558	0.19	0.71	0.54
Y23	364.7	Oil shale	140	52.1	64.4	118	93.7	567	0.17	0.73	0.55

(Continuation of Table 4)

Sample	Depth, m	Lithology	V, μg/g	Ni, μg/g	Cu, μg/g	Zn, μg/g	Sr, μg/g	Ba, μg/g	Sr/Ba	V/V+Ni	Cu/Zn
Y24	368.3	Siltstone	174	78	77.6	137	102	590	0.17	0.69	0.57
Y25	370.1	Oil shale	190	74.2	80.3	138	102	581	0.18	0.72	0.58
Y26	371.6	Muddy siltstone	144	48.1	73.1	108	115	654	0.18	0.75	0.68
Y27	372.5	Muddy siltstone	153	87.6	75	123	109	547	0.20	0.64	0.61
Y28	374.23	Mudstone	151	50.1	51.9	122	93.7	541	0.17	0.75	0.43
Y29	375.6	Oil shale	163	56.4	55.9	124	114	612	0.19	0.74	0.45
Y30	377.7	Muddy siltstone	155	54.8	53.5	134	92.9	521	0.18	0.74	0.40
Y31	379.7	Muddy siltstone	149	48.9	46.7	122	79.3	510	0.16	0.75	0.38
Coal-bearing Member											
Y33	476.1	Muddy siltstone	126	27.6	36.6	109	73.9	456	0.16	0.82	0.34
Y34	479	Oil shale	29.7	34.8	11.8	52	106	206	0.51	0.46	0.23
Y35	482.8	Muddy siltstone	124	55.4	21.3	120	28.8	50.1	0.57	0.69	0.18
Y36	492	Mudstone	108	33.3	45.4	69.1	101	237	0.43	0.76	0.66
Y37	494.7	Oil shale	47.8	19.7	27.6	25.4	140	274	0.51	0.71	1.09
Y38	497.7	Muddy siltstone	87.5	41.4	38.7	141	70.4	468	0.15	0.68	0.27
Y39	500.9	Siltstone	87	26	36.7	103	85.4	506	0.17	0.77	0.36
Y40	503.2	Muddy siltstone	99.5	16.6	38.1	130	90.7	502	0.18	0.86	0.29
Y41	506.2	Muddy siltstone	149	20.1	30.8	178	69.6	431	0.16	0.88	0.17
Y42	509	Muddy siltstone	88.3	42.9	29.5	111	137	383	0.36	0.67	0.27
Y43	516.8	Muddy siltstone	102	28.4	32	117	72.6	477	0.15	0.78	0.27
Y44	524.3	Muddy siltstone	102	32.1	32.6	130	102	483	0.21	0.76	0.25
Y45	529.5	Mudstone	118	34.4	28.3	79.7	72.2	494	0.15	0.77	0.36
Y46	534.3	Muddy siltstone	132	30.5	28.3	98.7	137	582	0.24	0.81	0.29
Y47	539.3	Muddy siltstone	98.2	29.3	28	109	142	566	0.25	0.77	0.26
Y48	542.84	Oil shale	61.9	30.3	46.9	32.6	593	1179	0.50	0.67	1.44
Y49	547.7	Coal	60.5	18	18.8	31.2	167	177	0.94	0.77	0.60
Y50	551.7	Oil shale	104	23.2	33.4	49.5	73.3	359	0.20	0.82	0.67
Y51	552.7	Silty mudstone	125	57.8	55.2	87.1	66.4	286	0.23	0.68	0.63
Y52	556.7	Silty mudstone	109	57.8	25.3	29	40	114	0.35	0.65	0.87
Y53	561.6	Muddy siltstone	89.4	27.6	34.5	110	61.9	383	0.16	0.76	0.31

In addition, the Ca/(Ca + Fe) ratio is also sensitive to changes in paleosalinity. A Ca/(Ca + Fe) > 0.8 implies salt water, and a value of 0.4–0.8 is a sign of brackish water. A ratio < 0.4 suggests fresh water [33]. The Ca/(Ca + Fe) ratio in the samples from J_2sh^1 also varied (Fig. 6d). The respective values of high-quality oil shale and coal samples were from 0.42 to 0.5, reflecting a brackish water environment, and those of poor-quality oil shale samples were between 0.14 and 0.27, indicating a fresh water environment (Fig. 6a and 6d). Similarly to Sr/Ba, the Ca/(Ca + Fe) ratio in the samples from J_2sh^2 was also very low at a depth from 380 to 352 m, all the values being lower than 0.4 (0.05–0.11), but the values increased toward the top and mostly exceeded 0.5 (Fig. 7a and 7e), reflecting that the lake water changed from fresh to brackish-salt.

These data indicate that high-quality oil shale and coal in J_2sh^1 and J_2sh^2 were deposited in a brackish to salt water environment, whereas poor-quality oil shale was deposited in a fresh water environment.

5.4.2. Redox conditions

Trace element ratios such as V/(V + Ni) and Cu/Zn have also been used as indicators to distinguish the redox environment. Generally, V/(V + Ni) ratios higher than 0.60 reflect anoxia, those between 0.46 and 0.60 mirror oxygen-depleted conditions, and ratios below 0.46 represent the oxic environment [34, 35]. The Cu/Zn ratio increases with decreasing oxygen availability [35]. V/(V + Ni) ratios of samples from J_2sh^1 ranged from 0.46 to 0.88 (average 0.74) (Table 4, Fig. 6e), implying an anaerobic environment. The Cu/Zn curve shows vertically three cycles, and the values for mudstone to oil shale samples in each cycle gradually increase, which is indicative of a step-by-step increase of reducing water (Fig. 6f). V/(V + Ni) ratios in the samples from J_2sh^2 were between 0.64 and 0.77 (average 0.71) (Table 4, Fig. 7f), while the Cu/Zn ratio increased with increasing oil yield (Fig. 7a and 7g). These data suggest that all samples from J_2sh^1 and J_2sh^2 were deposited in an anaerobic environment, and the reduction of lake water was stronger during deposition of high-quality oil shale.

The aforementioned trace element proxies show that water salinity and redox conditions control the preservation of organic matter. Brackish-salt water can easily form salinity stratification, making bottom water an anaerobic environment. In the anaerobic environment, the activity of micro-organisms and benthos is suppressed, and the degradation speed of organic matter by anaerobic bacteria is decreased, which remarkably contributes to OM preservation and high-quality oil shale formation.

6. Conclusions

Two oil shale sequences were identified in the Lower Coal-bearing Member and Upper Shale Member of the Middle Jurassic Shimengou Formation in

the Yuqia area of the northern Qaidam Basin, Northwest China. Bulk geochemical and proximate analyses revealed that the characteristics and accumulation conditions of the two types of oil shales were different.

1. Oil shale in J_2sh^1 mostly occurs with coal and carbonaceous shale. This oil shale with a high total organic carbon content (average 25.6 wt%) is dominated by Type II_2 kerogen (terrigenous organic matter). The oil shale of industrial quality has a medium-high oil yield (up to 10.4 wt%), low ash and moisture contents, and low-medium calorific value and sulfur content.

2. Oil shale in J_2sh^2 mostly occurs together with dark gray mudstone, silty mudstone and siltstone. Having a medium TOC content (average 8.0 wt%), this oil shale is dominated by Type I and II_1 kerogens (alginite and bituminite). The industrial-quality oil shale has a low-medium oil yield (up to 9.17 wt%), high ash content, and low moisture and sulfur contents and calorific value.

3. Major elements (Al_2O_3, K_2O/Na_2O, $CIA_{(molar)}$, CIA) and sedimentary facies analyses indicate that oil shale in J_2sh^1 was deposited in a limnic environment in a climate varying from warm-humid to hot-humid, whereas oil shale in J_2sh^2 was deposited in a semi-deep and deep lake environment in a stable warm-humid climate.

4. Typical trace element ratios (Sr/Ba, Ca(/Ca + Fe), V/(V + Ni), Cu/Zn) suggest that high-quality oil shale and coal in J_2sh^1 and J_2sh^2 were deposited in anaerobic, brackish to salt water, whereas poor-quality oil shale was deposited in fresh water.

5. Climatic conditions may control the quality, distribution and thickness of oil shale by influencing the formation of organic matter and the sedimentary environment. The stable warm and humid climate of J_2sh^2 easily formed a deep lake environment, benefiting lake paleoproductivity and depositing a thick layer of oil shale over a large area, whereas a varied climate and unstable limnic environment during the deposition of J_2sh^1 resulted in high terrigenous detrital matter input and the deposition of thin layers of oil shale over a small area. Under this scenario, high paleoproductivity during deposition of J_2sh^2 (or high terrigenous detrital matter input during deposition of J_2sh^1) and strong water salinity stratification were responsible for the accumulation of high-quality oil shale.

Acknowledgments

The authors would like to thank Professor of Engineering, Li Yonghong, from Qinghai Bureau of Coal Geological Exploration in Xining, Northwest China, for help in collecting the geological material and performing the field work in the Yuqia area. This research was supported by the China Geological Survey Scientific Research Project (1211302108025-3). The authors would also like to thank the two reviewers for their suggestions and comments that significantly improved the quality of the manuscript.

REFERENCES

1. Liu, Z. J., Meng, Q. T., Dong, Q. S., Zhu, J. W., Guo, W., Ye, S. Q., Liu, R., Jia, J. L. Characteristics and resource potential of oil shale in China. *Oil Shale*, 2017, **34**(1), 15–41.
2. Bechtel, A., Jia, J. L., Strobl, S. A. I., Sachsenhofer, R. F., Liu, Z. J., Gratzer, R., Püttmann, W. Palaeoenvironmental conditions during deposition of the Upper Cretaceous oil shale sequences in the Songliao Basin (NE China): implications from geochemical analysis. *Org. Geochem.*, 2012, **46**, 76–95.
3. Jia, J. L., Bechtel, A., Liu, Z. J., Strobl, S. A. I., Sun, P. C., Sachsenhofer, R. F. Oil shale formation in the Upper Cretaceous Nenjiang Formation of the Songliao Basin (NE China): implications from organic and inorganic geochemical analyses. *Int. J. Coal Geol.*, 2013, **113**, 11–26.
4. Xu, J. J., Liu, Z. J., Bechtel, A., Meng, Q. T., Sun, P. C., Jia, J. L., Cheng, L. J., Song, Y. Basin evolution and oil shale deposition during Upper Cretaceous in the Songliao Basin (NE China): Implications from sequence stratigraphy and geochemistry. *Int. J. Coal Geol.*, 2015, **149**, 9–23.
5. Song, Y., Liu, Z. J., Meng, Q. T., Xu, J. J., Sun, P. C., Cheng, L. J., Zheng, G. D. Multiple controlling factors of the enrichment of organic matter in the Upper Cretaceous oil shale sequences of the Songliao Basin, NE China: Implications from geochemical analysis. *Oil Shale*, 2016, **33**(2), 142–166.
6. Song, Y., Liu, Z. J., Bechtel, A., Sachsenhofer, R. F., Groß, D., Meng, Q. T. Paleoenvironmental reconstruction of the coal- and oil shale-bearing interval in the lower Cretaceous Muling Formation, Laoheishan Basin, northeast China. *Int. J. Coal Geol.*, 2017, **172**, 1–18.
7. Zhang, H. L., Liu, Z. J., Shi, J. Z., Meng, Q. T. Formation characteristics of oil shale in the Lower Cretaceous Dalazi Formation in the Luozigou basin. *Geology in China*, 2007, **34**(1), 86–91 (in Chinese, summary in English).
8. Guo, W., Zhang, Y. P., Li, Y. H., Jiang, T., Yang, H. X., Dang, H. L. Factors controlling the low radioactivity of oil shale in the 7th section of Dameigou Formation of Jurassic in northern Qaidam Basin. *Geoscience*, 2016, **30**(4), 905–913 (in Chinese, summary in English).
9. Ma, X. M, Hao, H. Y., Ma, F., Duan, G. L., Cheng, Y. H. Developmental value of oil shale in the 7th Member of Middle Jurassic in Yuqia area, Qaidam Basin. *Journal of Southwest Petroleum University (Science & Technology Edition)*, 2013, **35**(3), 52–58 (in Chinese, summary in English).
10. Zhou, F., Zhang, Y. S., Liu, Z. Q., Sui, G.., Li, G. J., Wang, C. X., Cui, S. K., Zhang, Y., Wang, J. R., Zhu, J. Geochemical characteristics and origin of natural gas in the Dongping–Niudong areas, Qaidam Basin, China. *J. Nat. Gas Geosci,*, 2016, **1**(6), 489–499.
11. Li, M., Shao, L. Y., Liu, L., Lu, J., Spiro, B., Wen, H. J., Li, Y. H. Lacustrine basin evolution and coal accumulation of the Middle Jurassic in the Saishiteng coalfield, northern Qaidam Basin, China. *J. Palaeogeogr.*, 2016, **5**(3), 205–220.
12. Liu, Z. J., Yang, H. L., Dong, Q. S., Zhu, J. W., Guo, W., Ye, S. Q., Liu, R., Meng, Q. T., Zhang, H. L., Gan, S. C. *Oil Shale in China*. Petroleum Industry Press, Beijing, 2009, 62–116 (in Chinese, summary in English).
13. Ren, Y. F., Chen, D. L., Kelsey, D. E., Gong, X. K., Liu, L. Petrology and geochemistry of the lawsonite (pseudomorph)-bearing eclogite in Yuka terrane, North Qaidam UHPM belt: An eclogite facies metamorphosed oceanic slice. *Gondwana Res.*, 2017, **42**, 220–242.

14. Dai, J. S., Ye, X. S., Tang, L. J., Jin, Z. J., Shao, W. B., Hu, Y., Zhang, B. S. Tectonic units and oil-gas potential of the Qaidam Basin. *Chinese Journal of Geology*, 2003, **38**(3), 291–296 (in Chinese, summary in English).
15. Shao, L. Y., Li, M., Li, Y. H., Zhang, Y. P., Lu, J., Zhang, W. L., Tian, Z., Wen, H. J. Geological characteristics and controlling factors of shale gas in the Jurassic of the northern Qaidam Basin. *Earth Science Frontiers*, 2014, **21**(4), 311–322 (in Chinese, summary in English).
16. GB/T 212-2008. Proximate analysis of coal. *The State Standards of the People's Republic of China*, 2008 (in Chinese).
17. GB/T 213-2008. Determination of calorific value of coal. *The State Standards of the People's Republic of China*, 2008 (in Chinese).
18. Taylor, G. H., Teichmuller, M., Davis, A., Diessel, C. F. K., Littke, R., Robert, P. *Organic Petrology*. Gerbrüder Borntraeger, Berlin-Stuttgart, 1998, 704.
19. GB/T14506.28-93. Methods for chemical analysis of silicate rocks. *The State Standards of the People's Republic of China*, 1994 (in Chinese).
20. DZ/T 0223-2001. Methods of inductively coupled plasma mass spectrometry ICP-MS analysis. *Recommended Standards for Geological Industry of the People's Republic of China,* 2002 (in Chinese).
21. Strobl, S. A. I., Sachsenhofer, R. F., Bechtel, A., Meng, Q. T., Sun, P. C. Deposition of coal and oil shale in NE China: The Eocene Huadian Basin compared to the coeval Fushun Basin. *Mar. Petrol. Geol.*, 2015, **64**, 347–362.
22. Zelenin, N. I., Ozerov, I. M. *Handbook on Oil Shale*. Nedra, Leningrad, 1983 (in Russian).
23. Lv, D. W., Li, Z. X., Liu, H. Y., Li, Y., Feng, T. T., Wang, D. D., Wang, P. L., Li, S. Y. The characteristics of coal and oil shale in the coastal sea areas of Huangxian Coalfield, Eastern China. *Oil Shale*, 2015, **32**(3), 204–217.
24. Yang, H. X., Yu, H. M., Li, P. W. Palaeomagnetic study of Qaidam plate and its evolution. *Journal of Changchun University of Earth Sciences*, 1992, **22**(4), 420–426 (in Chinese, summary in English).
25. Yang, P., Yang, Y. Q., Ma, L. X., Dong, N., Yuan, X. J. Evolution of the Jurassic sedimentary environment in northern margin of Qaidam basin and its significance in petroleum geology. *Petroleum Exploration and Development*, 2007, **34**(2), 160–164 (in Chinese, summary in English).
26. Nesbitt, H. W., Young, G. M. Early Proterozoic climates and plate motions inferred from major element chemistry of lutites. *Nature*, 1982, **299**, 715–717.
27. Goldberg, K., Humayun, M. The applicability of the chemical index of alteration as a paleoclimatic indicator: An example from the Permian of the Paraná Basin, Brazil. *Palaeogeogr. Palaeocl.*, 2010, **293**(1–2), 175–183.
28. Dymond, J., Suess, E., Lyle, M. Barium in deep-sea sediment: A geochemical proxy for paleoproductivity. *Paleoceanography*, 1992, **7**(2), 163–181.
29. Luo, Q. Y., Zhong, N. N., Zhu, L., Wang, Y. N., Qin, J., Qi, L., Zhang, Y., Ma, Y. Correlation of burial organic carbon and paleoproductivity in the Meso-proterozoic Hongshuizhuang Formation, northern North China. *Chinese Sci. Bull.*, 2013, **58**(11), 1299–1309.
30. Jones, B., Manning, D. A. C. Comparison of geochemical indices used for the interpretation of palaeoredox conditions in ancient mudstones. *Chem. Geol*., 1994, **111**, 111–129.
31. Shi, Z. S., Chen, K. Y., Shi, J., Liu, B. J., He, H. J., Liu, G. Feasibility analysis of the application of the ratio of strontium to barium on the identifying

sedimentary environment. *Fault-Block Oil & Gas Field*, 2003, **10**(2), 12–16 (in Chinese, summary in English).
32. Wang, M. F., Jiao, Y. Q., Wang, Z. H., Yang, Q., Yang, S. K. Recovery paleo-salinity in sedimentary environment - an example of mudstone in Shuixigou group, southwestern margin of Turpan-Hami basin, Xin Jiang. *Petroleum Geology*, 2005, **12**(6), 719–722 (in Chinese, summary in English).
33. Lan, X. H., Ma, D. X., Xu, M. G., Zhou, Q. W., Zhang, G. W. Some geochemical signs and their importance for sedimentary facies. *Marine Geology and Quaternary Geology*, 1987, **7**(1), 39–49 (in Chinese, summary in English).
34. Teng, G. E., Liu, W. H., Xu, Y. C., Chen, J. F. Correlative study on parameters of inorganic geochemistry and hydrocarbon source rocks formative environment. *Advances in Earth Sciences*, 2005, **20**(2), 193–200 (in Chinese, summary in English).
35. Wang, Y. Y., Guo, W. Y., Zhang, G. D. Application of some geochemical indicators in determining of sedimentary environment of the Funing Group (Paleogene), Jin-Hu Depression, Kiangsu Province. *Journal of Tongji University*, 1979, **7**(2), 51–60.

Presented by Ma Yue and A. Soesoo
Received April 25, 2017